International Journal of
MATERIALS RESEARCH

Zeitschrift für METALLKUNDE

Applied

Bevis Hutchinson[a], Matthew R Barnett[b], Alireza Ghaderi[b], Pavel Cizek[b], Ilchat Sabirov[b]
[a]SWEREA-KIMAB, Stockholm, Sweden
[b]CMFI, Deakin University, Geelong, Australia

Deformation modes and anisotropy in magnesium alloy AZ31

Dedicated to Professor Dr. Günter Gottstein on the occasion of his 65th birthday

A strongly textured sheet of magnesium alloy AZ31 has been subjected to tensile testing at temperatures between ambient and 300 °C. Structures have been examined by optical and transmission electron microscopy and also by atomic force microscopy to quantify surface displacements seen at grain boundaries. Plastic anisotropy varies strongly with test temperature as was observed previously by Agnew and Duygulu. The present findings do not support the view that crystallographic <*c* + *a*> becomes a major contributor to deformation at higher temperatures. Rather, the material behaviour reflects an increasing contribution from grain boundary sliding despite the relatively high strain rate (10^{-3} s^{-1}) used in the mechanical tests.

Keywords: Magnesium; Texture; Anisotropy; Slip systems; Grain boundary sliding

1. Introduction

Magnesium alloys are attractive as structural materials, especially in vehicles, because of their low density and high strength to weight ratios. However, most of these alloys exist in the close packed hexagonal structure which has important implications for their behaviour during plastic deformation. The strength, ductility and anisotropy of these materials have been subjects of study for many years in order to improve their formability during manufacturing and their strength in service [1–3]. At room temperature it is generally considered that the principal deformation modes are <*a*> slip on the basal plane and $\{10\bar{1}2\}\langle\bar{1}011\rangle$ twinning. These do not provide the five independent modes that are necessary for material continuity according to the von Mises principle; in particular, they make no provision for contraction along the *c*-axis. As a result, the ductility at room temperature is often limited. Other deformation modes such as prismatic <*a*> slip and other twinning systems may be activated at higher stress levels [4], for example providing some accommodation at grain boundaries, but the inadequacy of the common modes tends to dominate the mechanical properties of these materials. The restricted number of deformation modes also contributes to the development of sharp textures during processing by rolling or extrusion [5] and, furthermore, has the effect that these textures provide a high degree of mechanical anisotropy when the products are under stress in service [6–8].

The plastic behaviour of magnesium alloys changes considerably as the temperature is raised, [2, 7, 8]. In addition to the normal decrease in flow stress it was frequently found that the ductility increases markedly above about 200 °C and this has been attributed to reduction in the critical resolved shear stress (CRSS) for prismatic <*a*> slip which increases the number of independent deformation modes, although still not fulfilling the von Mises criterion. More recently, the effect of temperature has been studied in detail by Agnew and Duygulu [9] using a strongly textured AZ31 alloy where the *c*-axes were clustered close to the normal direction of the rolled plate. A combination of mechanical tests with transmission electron microscopy

(TEM) and computer analysis using viscoplastic self-consistent modelling (VPSC) demonstrated that prismatic <a> slip is a rather dominant process even at room temperature. A similar conclusion has also been reached in a study on slip lines [10]. In particular, prismatic <a> slip permits one to understand the high plastic strain ratios (R-values > 3) observed in tensile tests [9].

A particularly important observation of the work of Agnew and Duygulu [9] was that the R-values decreased to much lower values at elevated temperatures and were almost constant, in the range 1 to 1.5, above 200 °C. The conclusion from this work was of an increasing activity of $\{11\bar{2}2\}\langle 11\bar{2}3\rangle$ slip, often termed <c + a> slip, with temperature. As well as providing a convincing explanation for the R-value behaviour, the incorporation of <c + a> slip was consistent with texture changes during tension and evidence for the existence of these dislocations was found by TEM, confirming earlier claims of an important role of these <c + a> dislocations in magnesium [11, 12].

In addition to crystallographic slip, it has been found that gliding along grain boundaries takes place in magnesium at modestly elevated temperatures. Bell and Langdon [13] demonstrated the influence of grain boundary sliding (GBS) on the overall strain in creep tested Magnox alloy while Koike et al. [14] showed measurable GBS in tensile tests ($\dot{\varepsilon} \sim 10^{-3}\,s^{-1}$) even at room temperature and that this made a significant contribution to the total strain in an AZ31 alloy at 250 °C.

The present work was carried out with the principal aim of reviewing the role and importance of <c + a> slip at different deformation temperatures. An AZ31 alloy similar to that used by Agnew and Duygulu [9] was adopted because the variation of the plastic strain ratio had proved to be so revealing in their work.

2. Experimental procedure

The starting material was a commercially hot rolled 12 mm thick plate of AZ31 alloy containing 3.0 % aluminium and 0.8 % zinc as the only intentional elements in addition to magnesium. Pieces of this plate were further hot rolled in the laboratory at 300 °C to a final thickness of 4 mm with the aim of producing a sharp texture with the basal planes oriented close to the plane of the sheet (c-axes of the hexagonal lattice parallel to the sheet normal direction). Rolling was carried out in 5 passes with 15 minute re-heats between passes and without heating of the rolls. Most of the later experiments were carried out on the material in this hot rolled condition, which showed a very fine grained structure together with areas of heavily recovered substructure. From optical microscopy the grain size was estimated to be about 6 μm. Some samples were further annealed for 17 hours at 500 °C to generate a coarser grained structure, 38 μm grain size according to optical microscopy, for comparison purposes.

Microstructures and textures were examined by electron back-scattering diffraction (EBSD) using a Leo 1530 field emission gun scanning electron microscope (FEG-SEM) equipped with HKL Technology camera and software.

Tensile specimens were prepared from the transverse direction of the rolled sheet having a gauge length of 25 mm and a width of 5 mm. These were carefully ground to 2400 grade papers and then chemically polished in 10 % nital for 20 min to remove all traces of mechanical damage. Immediately after removing the specimens from this solution they were washed in an ultrasonic cleaner containing pure ethanol and dried. This procedure resulted in smooth clean surfaces suitable for metallographic observation, with no visible etching at the grain boundaries. Testing was carried out in a servo-hydraulic MTS machine equipped with an infra red lamp furnace that was controlled from a thermocouple in direct contact with the specimen surface. In most cases the initial strain rate was set at $10^{-3}\,s^{-1}$ but a few tests were carried out at higher and lower rates (10^{-2} and $10^{-4}\,s^{-1}$). Width and thickness measurements were made with a precision micrometer (accurate to 0.001 mm) initially and after the tests were stopped at a nominal 7 % permanent extension to evaluate the R-values. Based on the repeatability of these measurements the accuracy of the determined R-values is ±0.2.

Surfaces of the tensile specimens were examined using optical microscopy which indicated in some cases displacements along the grain boundaries after testing. Quantitative measures of these displacements were obtained from atomic force microscopy (AFM) using an Ultra Micro Indentation System (UMIS). The AFM scanning was carried out in contact mode with an applied force of 0.15 nN at a frequency of 294 kHz. The scanning areas varied from 10 × 10 μm to 30 × 30 μm in size. At least 10 successful scans were performed for each specimen. Dualscope/Rasterscope software from Danish Micro Engineering was used to reconstruct and analyse 3-dimensional digital elevation models of the scanned areas.

TEM was carried out on thin foils taken from tensile specimens tested at room temperature and 200 °C. Slices were cut perpendicular to the tensile axis and prepared by low energy ion beam milling before being examined in a Jeol JEM 2100 instrument operating at 200 kV. Initial grain orientations were determined from Kikuchi patterns using convergent beam electron diffraction. Using relatively small tilts it was possible to excite diffracting vectors of types (0002) and ($hki0$) which allow dislocations to be identified as <c + a> type or <a> type respectively. Several different areas were examined in this way from both test pieces.

3. Results and discussion

A representative EBSD micrograph of the hot rolled structure is shown in Fig. 1a. A majority of the material consists of recrystallised grains with sizes in the range from 3 to 15 μm but other areas were also present comprising well recovered subgrain structures. These features were confirmed in the higher resolution TEM images that are presented later. An analysis of grain size based on high angle boundaries with misorientations greater than 15° gave an average intercept length of 4.5 μm. The $\{0001\}$ and $\{10\bar{1}0\}$ pole figures are given in Fig. 1b and c where a Gaussian spread of 5° has been applied to the individual EBSD orientation measurements. It is seen that the texture is an almost perfect fibre with <0001> parallel to the normal direction of the sheet, having a full width half maximum (FWHM) spread of 36°. There is no evident preference for any crystallographic direction to align with the rolling direction; the a-directions of the crystals are distributed uniformly close to the plane of the sheet. The present texture resembles

quite closely that described in the experiments of Agnew and Duygulu [9] although there was some splitting of the central basal peak in their material and the peak intensity was somewhat less than here.

Flow stress values measured at 1 % and 5 % strain are shown as a function of tensile testing temperature in Fig. 2. As expected for this alloy, the strength decreases markedly with increasing temperature from room temperature to 250 °C. Optical microscopy showed that the grain structure was essentially unaffected in specimens tested up to 250 °C but there was evidence of some slight coarsening after testing at 300 °C. Subsequent analysis will therefore be restricted to temperatures from ambient to 250 °C. It is often explained that prismatic <a> slip and <c + a> slip are strongly thermally activated processes and so become increasingly influential in this temperature range as compared to basal <a> slip which behaves virtually athermally, [4]. At higher temperatures it is, therefore, expected that basal slip will become less significant and, as well as reducing the flow stress, a change in the alloy's anisotropy may be expected.

A change in the anisotropy is clearly seen in the *R*-value measurements plotted in Fig. 3. At room temperature the *R*-value has the high value of 3.7 but decreases slightly at 100 °C and then very rapidly to 150 °C. At and above 200 °C the value is about 1.3 and is approximately constant. The present anisotropic behaviour is in good accordance with measurements of Agnew and Duygulu [9] for their tests along the transverse direction, which are shown by the dashed line in Fig. 3. Those values are somewhat

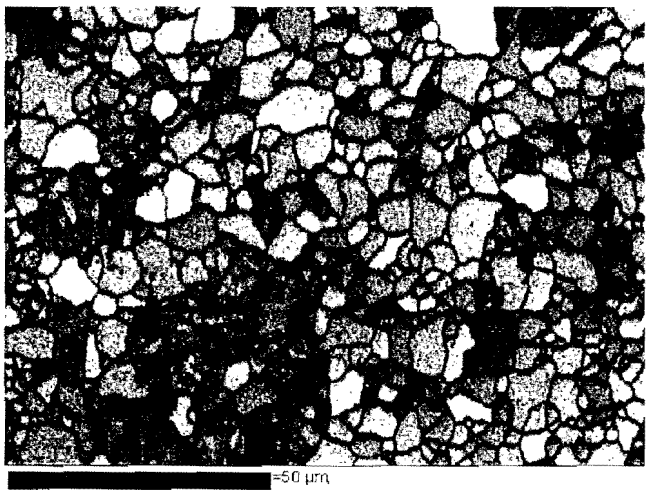

(a)

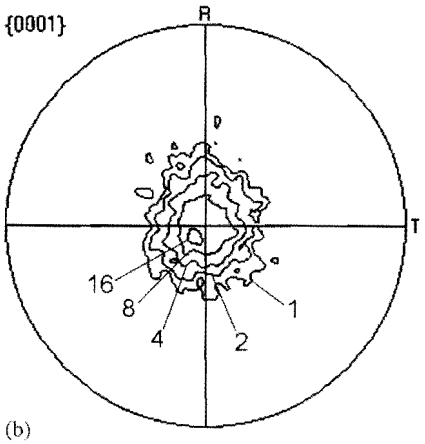

(b)

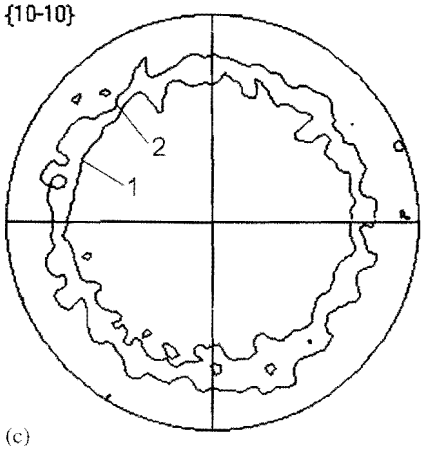

(c)

Fig. 1. Microstructure and texture of the hot rolled AZ31 alloy. (a) EBSD map, (b) {0001} pole figure, (c) {10$\bar{1}$0} pole figure.

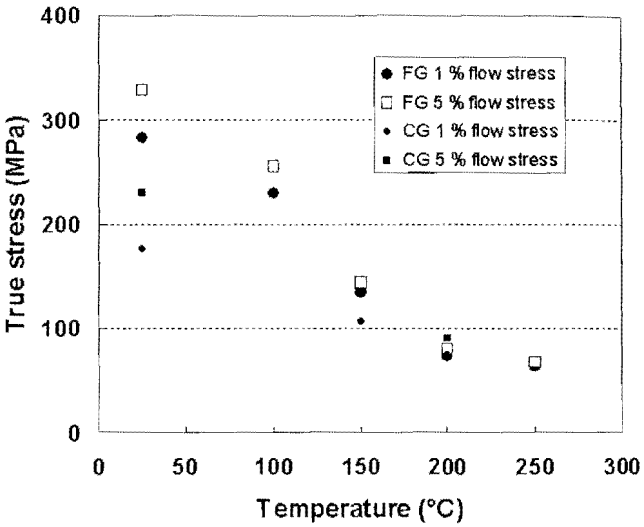

Fig. 2. Flow stress values at 1 % and 5 % plastic strain for AZ31 alloy tested in tension at different temperature. Large symbols show hot rolled, fine grained condition (FG) and small symbols are for the annealed coarse grained condition (CG).

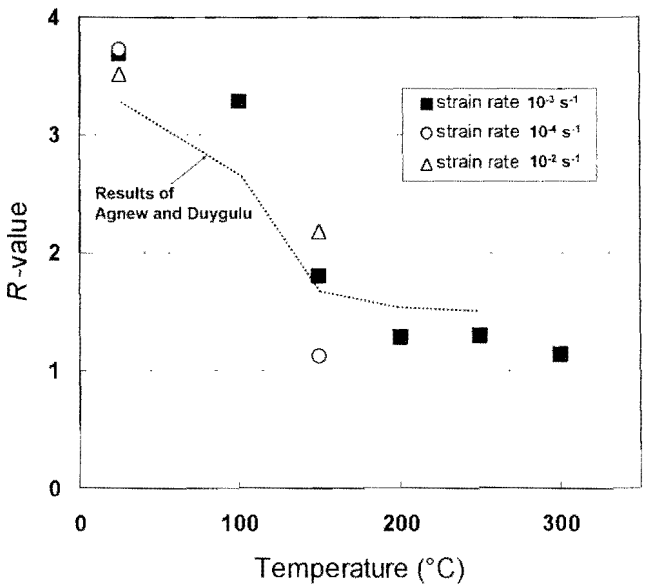

Fig. 3. *R*-values for hot rolled AZ31 alloy tested in tension at different temperatures. Data from Agnew and Duygulu [9] are shown for comparison.

smaller at the lower temperatures than ours which is not unreasonable in view of the sharper texture in the present material. Some results at different strain rates are also included in Fig. 3. For room temperature tests there is no evident influence of testing speed but at 150 °C the R-values systematically decrease with reduction in applied strain rate. This is a type of behaviour that can be understood on the basis that thermally activated processes are at work so that time and temperature can compensate for one another in their respective influences on the deformation modes.

Optical metallography carried out on the surfaces of the tensile specimens showed significant differences depending on the testing temperature. In Fig. 4 micrographs are shown for four different conditions. At room temperature, Fig. 4a, there is some undulation at the surface resulting from the underlying plastic deformation but only very few areas contained slip bands so it was not possible to deduce directly the active slip modes in this case. After straining at 100 °C, Fig. 4b, the surface was generally similar although occasional marks were present along some of the grain boundaries. These grain boundary signatures became increasingly evident at higher temperatures, Fig. 4c and d, with a tendency for the boundary traces lying perpendicular to the tensile axis to be most prominent. It was clear that these marks were the result of surface steps that appeared due to sliding in the grain boundaries, in particular along boundaries that had experienced the greater levels of shear stress during the tensile loading.

Quantitative measurements of the displacements at grain boundaries were obtained with good precision using AFM. An example of one of these surfaces is shown in Fig. 5a and b and the corresponding surface topography profile is given in Fig. 5c. It is evident that shearing had occurred parallel to the grain boundaries. The regular striations which can be seen on the exposed grain boundary surfaces in Fig. 5a are an artefact from the scanning raster in the AFM. For the present purposes, the exact mechanism for shearing is not critical; the important aspect is that the geometry of deformation is defined by the physical grain boundary network rather than the crystal orientations inside the grains. Average height displacements where boundary sliding occurred at the specimen surface obtained from AFM are summarised in Table 1. No clear values could be measured for room temperature and 100 °C tests but the vertical displacements increased progressively at higher testing temperatures.

As mentioned previously, the 300 °C test showed evidence of grain boundary migration and grain growth so this is not considered to be equivalent to the others where the grain structures were essentially constant during the deformation.

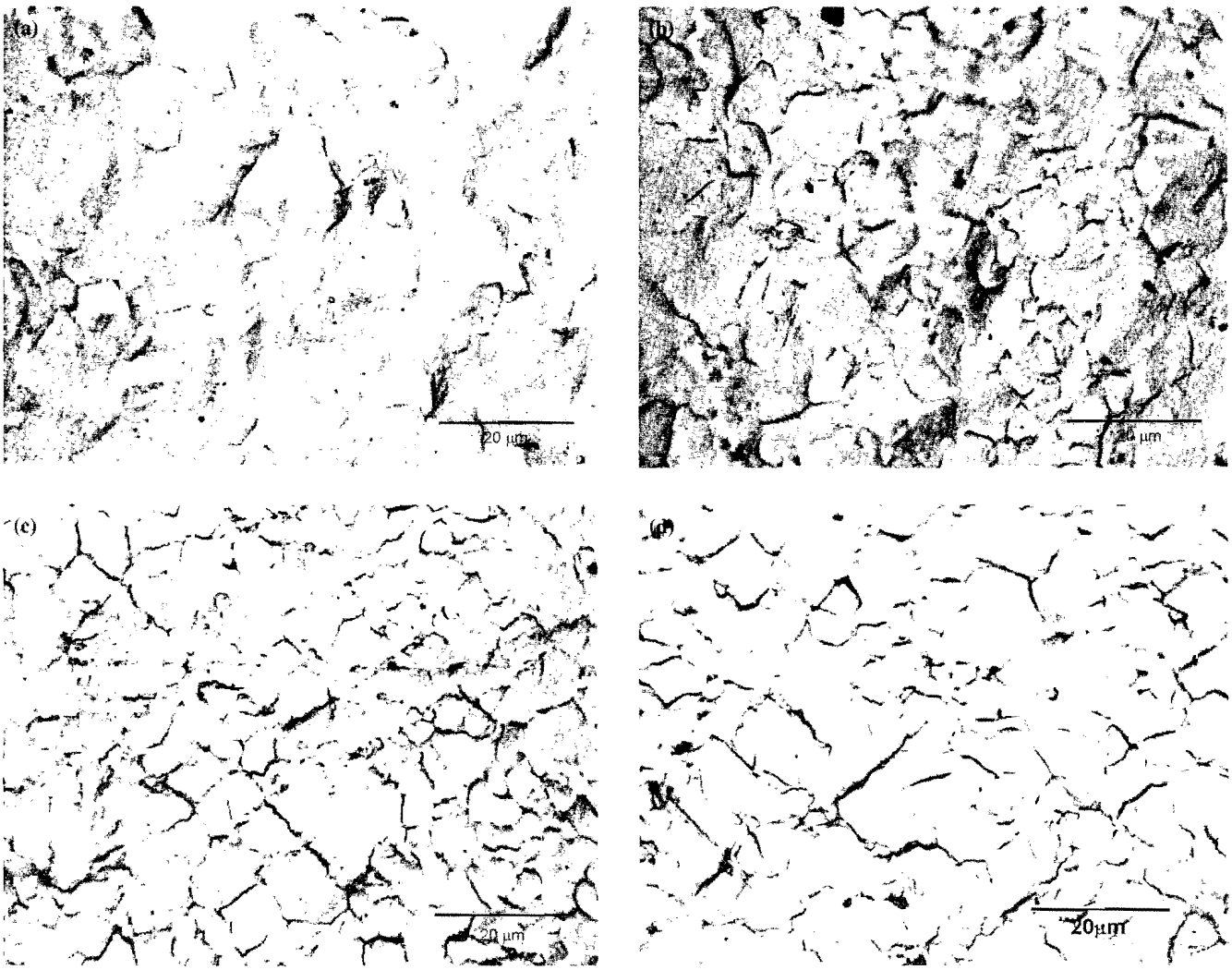

Fig. 4. Optical micrographs of surfaces of tensile specimens tested at different temperatures, (a) room temperature, (b) 100 °C, (c) 150 °C, (d) 200 °C.

Dislocation analyses were carried out using TEM on specimens tested at room temperature and at 200 °C. These were the same specimens on which the R-values had been measured, having plastic strains of 6.8 % and 6.3 % respectively. Eight different grains were examined in the former case and ten grains in the latter. Orientations of the foil normal directions in these grains, which correspond to the tensile axis, are shown in Fig. 6a and b and confirm the sharp fibre texture of the material. All these directions lie close to the basal plane but they are quite uniformly spread in that plane. The dislocation character was determined from diffraction with $\boldsymbol{g}$ vectors {0002} for which all <a> dislocations are invisible but all <$c + a$> are visible, together with either $\{10\bar{1}0\}$ or $\{11\bar{2}0\}$ which reveal all <$c + a$> dislocations as well as most <a> dislocations. We have not attempted to determine the precise Burgers vectors since previous experience, Jones and Hutchinson [15], has confirmed the general reliability of this method for identification but also showed that a totally rigorous proof of dislocations' <$c + a$> character by $\boldsymbol{g} \cdot \boldsymbol{b}$ analysis can be problematic due to residual contrast with some diffracting vectors.

Figure 7a and b shows a region from a specimen deformed at room temperature. The presence of visible dislocations with $\boldsymbol{g} = \{11\bar{2}0\}$ and their absence with $\boldsymbol{g} = \{0002\}$ show that only <a> type dislocations exist here. These dislocations, as well as other similar ones that were observed, tended to be straight or only slightly curved and were projected approximately parallel to the basal plane. For this grain orientation, prismatic slip should be favoured. Thus, it seems that prismatic slip, if present, may largely occur as cross slip from the basal plane as suggested by Couret and Caillard [16]. A different region from the same specimen, Fig. 7c and d, however, has visible dislocations for both $\{10\bar{1}0\}$ and {0002} diffracting vectors. Here there are both <a> and <$c + a$> dislocations present. The latter were sometimes strongly curved as in Fig. 7d but more commonly were quite straight.

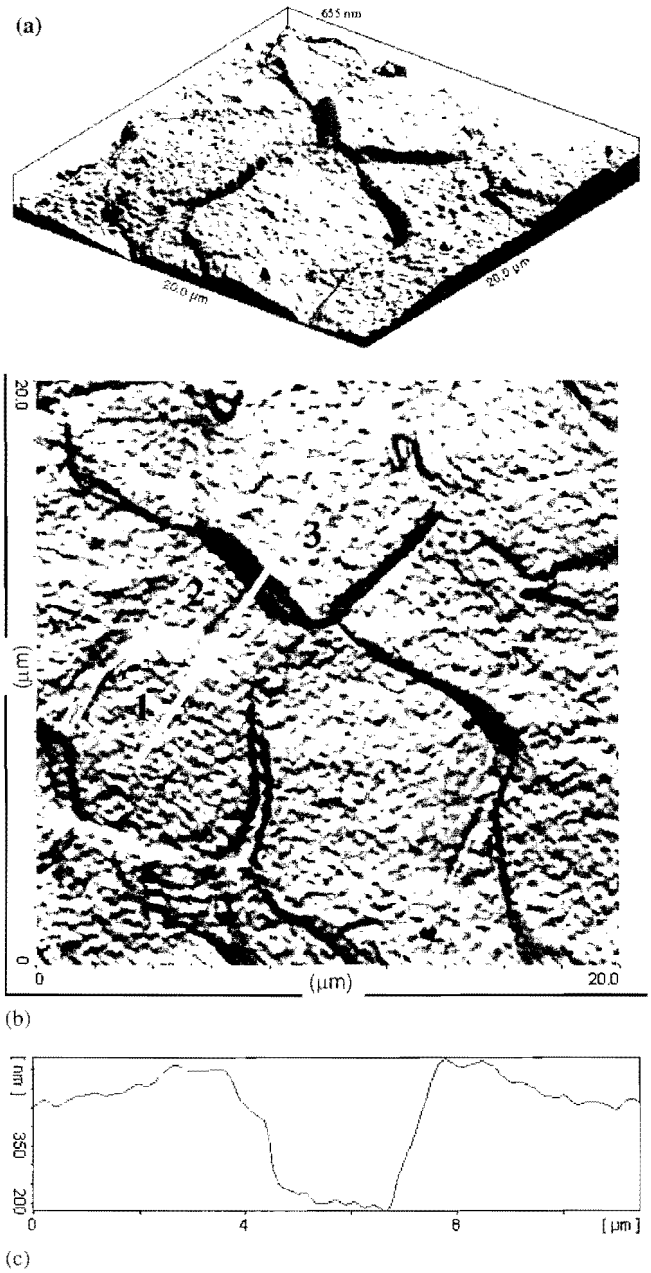

Fig. 5. AFM results from the surface of a tensile specimen tested at 250 °C, (a) 3-dimensional representation, (b) 2-dimensional plot, (c) surface profile across two grain boundaries.

Table 1. Average vertical step height at grain boundaries after tensile straining at different temperatures.

Temperature (°C)	25	100	150	200	250	300
Axial tensile strain %	6.77	7.75	6.23	6.25	5.64	12.67
Average step height (nm)	0	0	141	212	227	342

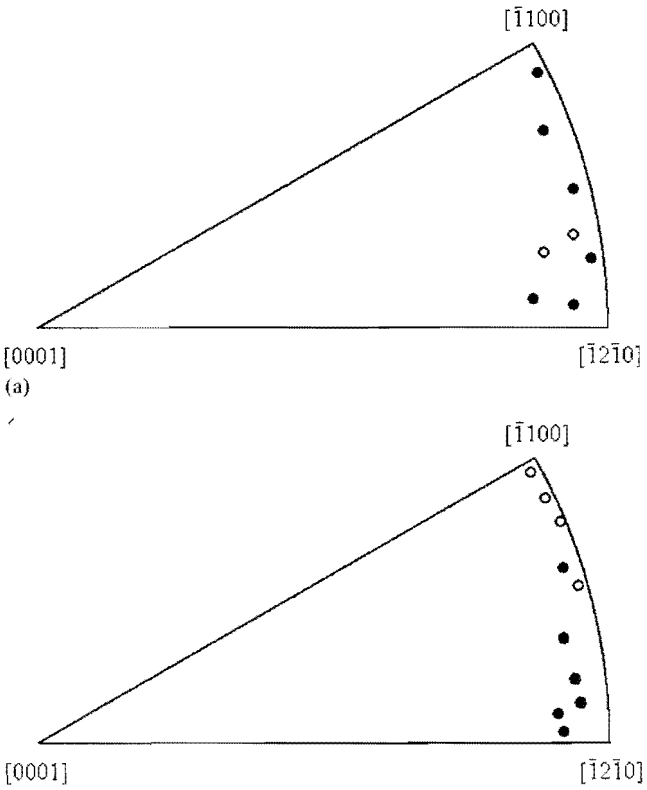

Fig. 6. Foil normals of grains examined by TEM. Solid symbols – grains having only <a> dislocations; open symbols – grains having both <a> and <$c + a$> dislocations. (a) specimen deformed at room temperature, (b) specimen deformed at 200 °C.

Generally similar behaviour was observed in the specimen that was strained at 200 °C. Most of the grain shown in Fig. 7e and f contains only <*a*> dislocations but in some localised regions, Fig. 7 g and h, <*c* + *a*> dislocations were also found. Other grains were similar in containing either only <*a*> dislocations or these together with localised small clusters of <*c* + *a*> type.

Well recovered sub-boundaries were also seen, shown by arrows in some grains. These are believed to be remnants of deformation structure produced during the hot rolling as had been indicated by the EBSD results. From the present TEM studies there was little difference to be seen between the dislocation structures produced by straining at room temperature or 200 °C. In Fig. 6 the grains containing <*c* + *a*> dislocations are shown as open symbols while those having only <*a*> type have closed symbols. For room temperature tests, two of the eight grains contained <*c* + *a*> dislocations as compared to four out of ten grains for 200 °C. In most cases these constituted a small minority and the <*a*> dislocations were generally dominating for both deformation temperatures.

In view of the tendency for grain boundary sliding that was seen to occur above about 100 °C, some further experiments were carried out on the alloy after annealing to increase the grain size and, therefore, to reduce the tendency for grain boundary effects. Annealing for 17 h at 500 °C resulted in a uniform grain structure with an average intercept length of 38 μm, or some eight times larger than the as hot rolled condition. Pole figures in Fig. 8 show that the texture after annealing was the same basal fibre type as previously but somewhat stronger and narrower, having a FWHM value of 32°. Such a sharpening of the recrystallised texture during subsequent grain growth is commonly observed in metals and alloys [17]. Due to the limited amount of material, tensile tests were done only at room temperature, 150 °C and 200 °C. Flow stresses for these specimens are shown with smaller sized symbols in Fig. 1. At room temperature and 150 °C the annealed alloy is less strong than it is in the initial hot rolled state which could be expected from the larger grain size and also the elimination of recovered substructure. However, at 200 °C this annealed condition is actually slightly stronger which supports the idea that de-

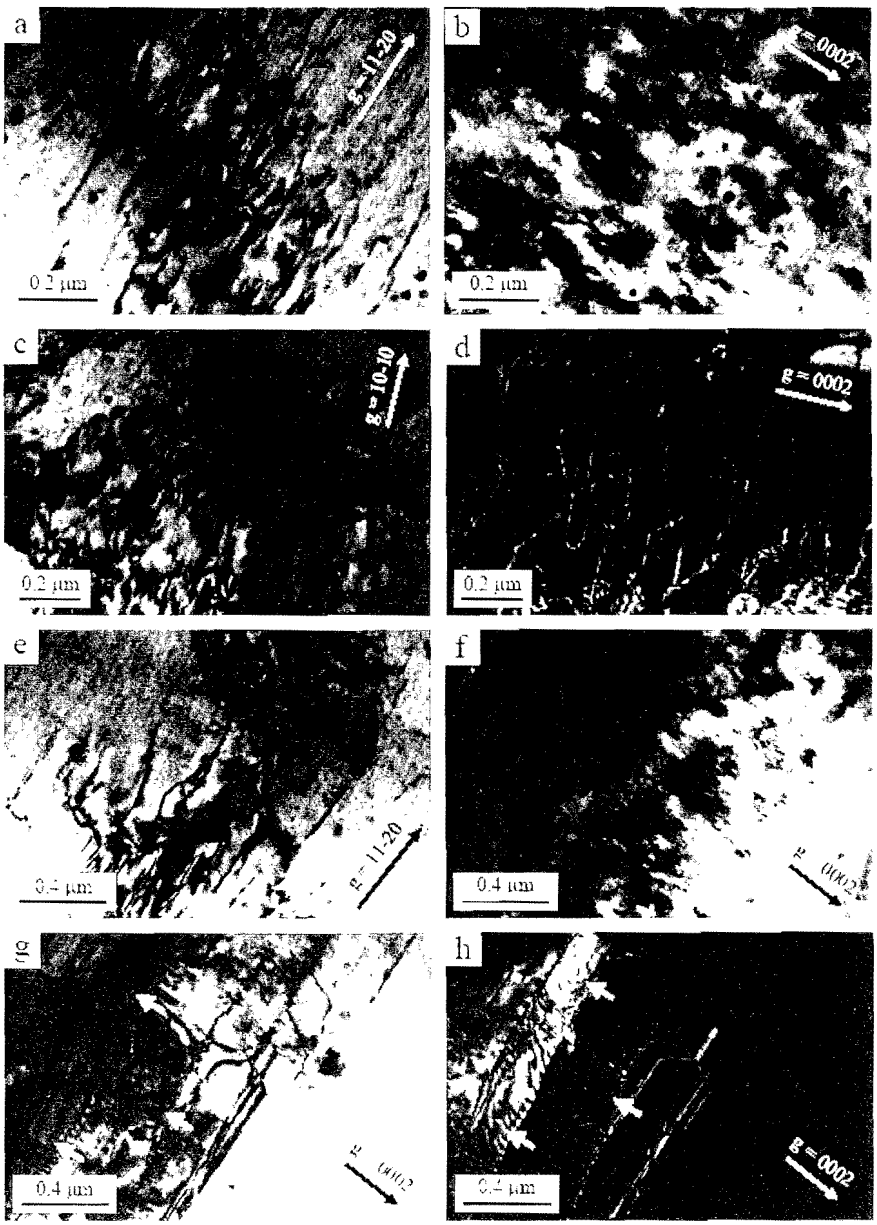

Fig. 7. TEM images of dislocations in specimens strained in tension, (a)–(d) at 25 °C and (e)–(h) at 200 °C. Pairs of images from the same areas are shown with different diffracting conditions in (a)&(b), (c)&(d), (e)&(f) and (g)&(h). Images shown are in bright field except for (d) and (h) which are in weak-beam dark field. Some low angle boundaries from prior processing are indicated by arrows.

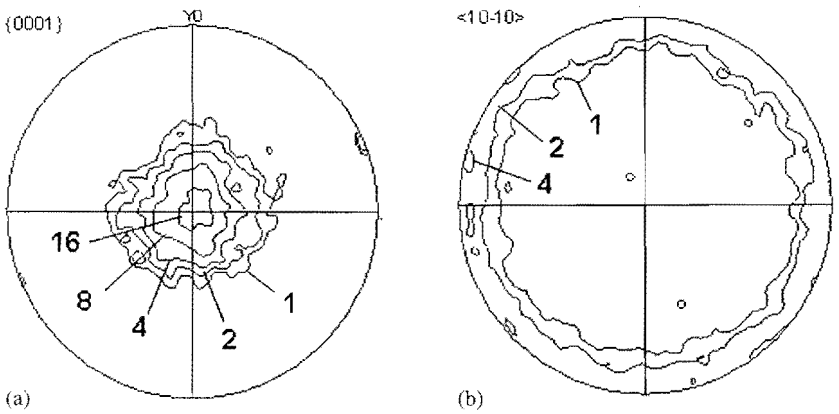

Fig. 8. (a) {0001} and (b) {10$\bar{1}$0} pole figures for the alloy after annealing 17 h at 500 °C in order to generate a coarser grained structure.

Table 2. *R*-values for the alloy at different testing temperatures.

Alloy condition	Grain size	*R*-value 25 °C	*R*-value 150 °C	*R*-value 200 °C
As hot rolled	4.5 μm	3.69	1.80	1.29
Annealed 500 °C/17 h	38.2 μm	4.25	4.42	3.36

formation processes occurring at the grain boundaries may be of major importance. Further support for this view is seen in the *R*-values summarised in Table 2.

The room temperature *R*-value for the annealed sheet is higher than for the as hot rolled condition which is in accordance with its stronger basal texture. The value at 150 °C is actually higher than that at room temperature but they may be considered equal within the uncertainty of the measurements. Only a modest decrease is seen at 200 °C and the *R*-value is still at a remarkably high level compared to the fine grained hot rolled condition which is nearly isotropic at this temperature.

4. General discussion

The present work was inspired by the report of Agnew and Duygulu [9] and reproduces quite well some of their most significant observations although we come to a rather different conclusion concerning the deformation mechanism. Their material had a different processing history, being in a cold rolled and recovery annealed state (H24 temper) whereas ours was hot rolled. Nevertheless, both should have fine scale microstructures and the textures were rather similar. In making comparison with their tensile test results we concentrate on those in the transverse direction where the anisotropy was greatest and the influence of temperature was most evident. In fact, the anisotropy and temperature dependence of the present alloy was even more pronounced, Fig. 3, probably due to the stronger and more perfect basal texture. As pointed out previously [9], such a decrease in *R*-value cannot be due to enhanced slip activity on prismatic planes with increasing temperature, as was often assumed to occur, since this should have the opposite effect of increasing *R* and so $<c + a>$ slip was put forward as an alternative explanation.

The TEM observations summarised in Fig. 7 show that both $<a>$ and $<c + a>$ slip take place during deformation at room temperature as well as at 200 °C. It is possible that $<c + a>$ becomes more prevalent at the higher temperature where these dislocations were seen in four of the ten grains (40 %) examined as compared to two out of eight grains (25 %) at room temperature. However, the statistics are poor in this regard and, even when present, the $<c + a>$ dislocations were not widespread but appeared rather to occur for reasons of local accommodation. The TEM results do not make a convincing case for $<c + a>$ slip as a major deformation mode at either temperature. This conclusion is also in conformity with the findings of Gehrmann et al. [8] which were based on modelling of the texture evolution.

Evidence for grain boundary sliding as a significant deformation mode appeared in the optical microscopy, Fig. 4, and is seen still more clearly in the AFM results in Fig. 5. Koike et al. [14] reported that GBS could contribute up to 27 % of the plastic strain that occurred in their tensile tests at 250 °C. The contribution made by GBS to axial strain has been reviewed by others, for example, by Stevens [18]. Height displacements at surface steps can give a good measure of this, especially when these can be measured accurately with AFM as here. Since the structure is equi-axed, the axial strain due to GBS is proportional to the average step height and inversely proportional to the average grain intercept length with a proportionality constant close to unity. Also, since the structure is equi-axed, the lateral strain ratio (*R*-value) associated with deformation by GBS should be unity. It is, therefore, possible to compute the to-

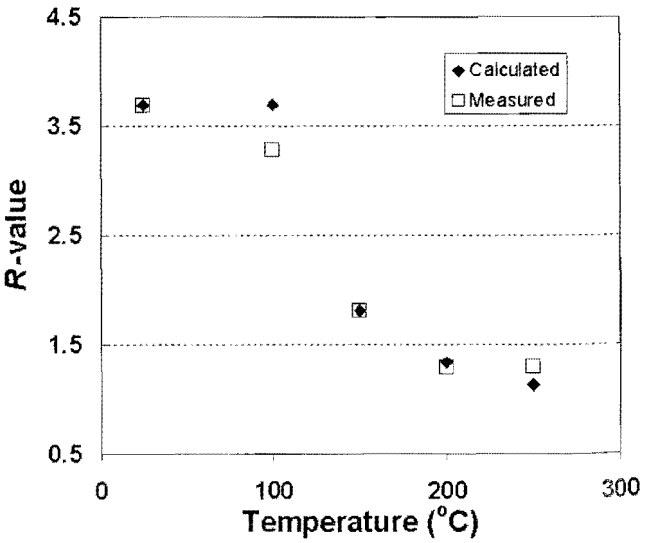

Fig. 9. Comparison of *R*-values for the hot rolled alloy from direct measurement and from calculations based on a combination of intragranular slip processes and grain boundary sliding.

tal R-value from the combination of GBS and intra-granular plastic deformation. We assume here that the deformation inside the grains gives rise to the same R-value at all temperatures (no change in the crystallographic slip modes) and also that the two sources of deformation act independently of one another. The intra-granular strain ratio is taken to be that at room temperature where GBS is negligible, while other inputs are also measured values. The axial strain due to GBS is first calculated and deducted from the total measured strain leaving a residue which is the intra-granular strain. Figure 9 shows the results of these calculations for the hot rolled sheet as compared with the measured R-values at different test temperatures. Notwithstanding the assumptions made and uncertainty in measured data, the agreement between theory and experiment is very close. The small discrepancy at 100 °C is apparently due to the failure to recognise sliding in the AFM measurements although some indications did appear in the optical micrographs, Fig. 4b.

Grain boundary sliding is known to be markedly dependent on deformation speed and the strain rate sensitivity index (m) for tensile tests shows a relatively high value around 0.1 at 150 °C [9]. It was also seen here that the R-value at that temperature varied strongly with testing speed, being smaller for slow strain rates. Although not constituting proof, this is further supporting evidence that GBS may be involved.

Probably the most convincing evidence of all for the role of GBS as the alternative to $<c + a>$ slip at elevated temperatures comes from the limited results for the annealed coarse grained alloy, Fig. 1 and Table 2. Flow stress data show that the strengthening effect of the fine grain structure is lost progressively with increasing temperature of deformation, becoming negative at 200 °C, as the grain boundary regions get softer relative to the grain interiors. More significantly, the plastic anisotropy in the coarser grained material is little affected by temperature. There is no good reason to believe that changing the grain size should influence dramatically the active slip systems but the contribution to total strain from GBS will be progressively reduced as grain size increases. Some effect of GBS must remain, of course, even in coarse grained material and this is most probably the explanation for the somewhat lowered R-value in the 200 °C test. Assuming that the displacements due to GBS are the same as for the fine grained material at this temperature, a similar calculation to the one above predicts the value of R in the coarse grained case to be 3.67 as compared to the measured value of 3.36.

The aim of this work was principally to understand the plastic anisotropy of the present alloy and in particular its temperature dependence. To summarise, it is clear that $<c + a>$ slip does occur in this alloy under the conditions of our tests. However, the TEM observations showed that the majority of grains (12 out of the 18 studied) do not contain these dislocations and, accordingly, they cannot play a major role in the total deformation. It is possible that $<c + a>$ slip becomes slightly more prevalent with increasing temperature but this cannot be stated with certainty. Based on several different observations, there appears to be a high degree of certainty that the changes in plastic anisotropy above room temperature are not due to a stronger influence of $<c + a>$ slip but result instead from incursion of grain boundary sliding.

5. Conclusions

Experimental findings of the present work are in good accord with results reported in the literature for similar materials. In particular, the strong influence of testing temperature on plastic anisotropy of textured AZ31 alloy is confirmed. However, there is little evidence for significant increase in the activity of $<c + a>$ slip at higher temperatures. The behaviour of the material becomes modified by the incursion of grain boundary sliding as a major deformation mode despite the relatively high strain rate (10^{-3} s^{-1}) that was used. Grain size has, therefore, an important role in the mechanical behaviour of this and similar magnesium alloys.

WBH wishes to thank Deakin University and the ARC Centre of Excellence for Design in Light Metals for providing facilities and financial support during this work.

References

[1] A. Beck: The technology of magnesium and its alloys, FA Hughes, London (1940).
[2] C.S. Roberts: Magnesium and its alloys, John Wiley and Sons, New York (1960).
[3] S.R. Agnew, M.H. Yoo, C.N. Tomé: Acta Mater. 49 (2001) 4277–4289.
[4] R.E. Reed-Hill: Deformation twinning, Gordon and Beach, New York (1964).
[5] M.J. Philippe: Mater. Sci. Forum 157–162 (1994) 1337–1350.
[6] E.W. Kelly, W.F. Hosford: Trans. Met. Soc. AIME 242 (1968) 654–660.
[7] B.C. Wonsiewicz, W.A. Backofen: Trans. Met. Soc. AIME 239 (1967) 1422–1431.
[8] R. Gehrmann, M.F. Frommert, G. Gottstein: Mater. Sci. Eng. A 395 (2005) 338–349.
[9] S.R. Agnew, O. Duygulu: Int. J. Plasticity 21 (2005) 1161–1193.
[10] Z. Keshavarz, M.R. Barnett: Scripta Mater. 55 (2006) 915–918.
[11] J.F. Stohr, J.P. Poirier: Phil. Mag. 25 (1972) 1313–1329.
[12] T. Obara, H. Yoshinaga, S. Morozumi: Acta Metall. 21 (1973) 845–853.
[13] R.L. Bell, T.G. Langdon: J. Mater. Sci. 2 (1967) 313–323.
[14] J. Koike, R. Ohyama, T. Kobayashi, M. Suzuki, K. Maruyama: Mater. Trans. 44 (2003) 445–451.
[15] I.P. Jones, W.B. Hutchinson: Acta Met. 29 (1981) 951–968.
[16] A. Couret, D. Caillard: Phil. Mag. 63 (1991) 1045–1057.
[17] W.B. Hutchinson, E. Nes: Mater. Sci. Forum 94–96 (1992) 385–390.
[18] R.N. Stevens: Trans. Met. Soc. AIME 236 (1966) 1762–1764.

(Received August 25, 2008; accepted January 1, 2009)

Bibliography

DOI 10.3139/146.110070
Int. J. Mat. Res. (formerly Z. Metallkd.)
100 (2009) 4; page 556–563

ISSN 1862-5282

Correspondence address

Prof. Bevis Hutchinson
Swerea-Kimab
PO Box 55970, SE-10216 Stockholm, Sweden
Tel.: +46 8 440 4888
Fax: +46 8 440 4535
E-mail: bevis@kimab.com